



Development of Myelinating Human Brain Organoids for Modelling Multiple Sclerosis: A Platform For Drug Screening Studies and Mechanistic Investigations

Büşra Acar¹, Alaattin Şen^{1,2*}

¹Department of Molecular Biology and Genetics, Faculty of Life and Natural Sciences, Abdullah Gul University 38080 Kayseri, Türkiye

²Department of Biology, Faculty of Sciences, Pamukkale University, 20070 Kinikli, Denizli, Türkiye

Cite: Acar B., Şen A. Development of myelinating human brain organoids for modelling multiple sclerosis: a platform for drug screening studies and mechanistic investigations. *Eurasian Mol Biochem Sci* 2025;4(2): 64-76

Received: 22 May 2025, Accepted: 5 August 2025

DOI: 10.5281/zenodo.17786373

Abstract

Multiple sclerosis (MS) is a neurodegenerative disease that is characterized mainly by demyelination and inflammation. The disadvantages of the current two-dimensional cell culture models and experimental animals imply the need for the development of new disease models. Brain organoids are emerging and powerful tools for recapitulating the central nervous system. Although the models have been generated for many years, time-consuming processes and less cellular diversity are important challenges in defined protocols. In this study, we aimed to generate an optimized brain organoid protocol and model organoids for MS. In these processes, human embryonic stem cells were directed to neurons via the extracellular matrix (ECM) and growth factors to generate brain organoids with diverse neural cells. The presence of myelinating cells, astrocytes, microglia and excitatory neurons in the organoids was verified by immunostaining. MS was then used to induce inflammation and demyelination via lipopolysaccharide (LPS). The model was also confirmed by immunostaining, which revealed an ~50% increase in GFAP and an ~60% decrease in CNPase-positive cells. Finally, the use of organoids in the drug screening field was tested via fingolimod treatment of LPS-induced organoids. A comparison between fingolimod-treated and untreated organoids revealed that fingolimod decreased GFAP by more than 80% and increased the percentage of CNPase-positive cells by 90%. Additionally, the relative expression levels of inflammation-related transcripts (FOXP3 and GFAP) after fingolimod treatment were significantly decreased. In conclusion, a human brain organoid model for MS studies was successfully generated for use in drug screening and mechanistic studies.

Keywords: Brain organoids, myelination, inflammation, multiple sclerosis

***Correspondence:** Alaattin Şen
Department of Biology, Faculty of Sciences,
Pamukkale University, 20070 Kinikli, Denizli, Türkiye
E-mail: alaattinsen422261@gmail.com
Tel: +90-532-761-3356



Introduction

Neurodegenerative diseases are multifactorial, and several of them are affected by immune system dysfunction, whereas others result in myelin sheath disruption. Multiple sclerosis (MS) is an autoimmune disease characterized by myelin loss around axons in the central nervous system (1,2). MS causes an abnormal immune response leading autoreactive cells pass the blood-brain barrier, which damages myelin sheaths and axons. This results in impaired neuronal signal and neurological problems. Disease-modifying therapies (DMTs) are employed to manage multiple sclerosis (MS) by diminishing CNS infiltration and inflammation and decelerating disease progression through the modulation of inflammatory and immunological responses in affected individuals, rather than offering a definitive cure for the condition (3). fingolimod (FTY720, Gilenya), a synthetic derivative of sphingosine, was the first disease-modifying therapy licensed by the Food and Drug Administration for the oral treatment of multiple sclerosis. Upon phosphorylation, it is associated with sphingosine-1-phosphate receptors (S1PRs), leading to the internalisation and destruction of S1PR1. Consequently, fingolimod diminishes both T and B lymphocytes in the bloodstream and those that infiltrate the central nervous system. (4,5). Despite advances in neuroimmunology studies, the molecular and cellular mechanisms underlying the pathology of this disease are not fully understood (6). Therefore, recapitulating the cytoarchitecture of the human brain is highly important for revealing disease pathophysiology and enhancing treatment (7). Compared with two-dimensional cell culture systems and animal facilities, brain organoids are remarkable tools for mimicking human physiology. They are three-dimensional cell culture systems that are derived from stem cells to be directed into neurons with the help of the extracellular matrix and growth factors (8).

Organoids are a relatively emerging area for creating organ models; however, they have advantages over traditional cell culture models and animal usage. Although animal models have been used to model many diseases for many years, they do not accurately reflect human physiology. Additionally, the ease of system establishment and maintenance, genetic manipulation, lack of genome-wide screening, and cost make animals less preferable for studying human neurodevelopmental and neurodegenerative diseases (8). Compared with animal models and organoids, two-dimensional cell culture models offer a shorter experimental duration and lower cost; however, the lack of cell–cell and cell–environment interactions, lack of compartmentalization, and physiological complexity make them a less preferred system. For example, neurons in monolayer culture are easily genetically manipulated and differentiated; however, differentiated cells cannot segregate into different layers to form different brain compartments (8,9). Therefore, compared with traditional culture methods and animal models, organoids hold great promise for studying diseases (8,10). In the literature, some notable studies have attempted to create a model for neurodegenerative diseases (11). Even though some pacesetter studies modelling MS on organoids, only oligodendrocytes or only the microglial cell population were shown on the organoids (12,13). However, MS is a disease characterized by inflammation and demyelination, and there are no reported studies showing an inflammatory demyelinated brain organoid model. In contrast to encouraging studies regarding MS modelling, the lack of oligodendrocytes and myelin wrapping are two of the important challenges in brain organoid modelling for neurodegenerative diseases because of the extra support necessity for oligodendrocyte generation. Although there is no well-defined and consensus brain organoid model for generating a disease model characterized by myelin

loss (7), it has also been reported that clemastine and ketoconazole-like myelination-enhancing molecules contribute to the increase in the number of myelinating organoids; however, the processes either take approximately 210 days or generate only myelinating cells and astrocytes, not microglia (14-16). Such extended time requirements and a lack of cellular diversity make the previous protocol impractical. In addition to the studies showing myelinating cells, some studies focused on the generation of an inflammatory cell population in brain organoids, but not oligodendrocytes (17). Therefore, in this study, it is aimed to generate myelinating brain organoids model with various neural cell populations, including astrocytes, myelinating cells and microglia, in a reasonable duration. And confirming the functionality of the model with fingolimod, a well-known disease modifying drug currently used for MS.

Materials and Methods

Feeder-dependent and feeder-independent culture of human embryonic stem cells: For organoid generation, H9 cells (human embryonic stem cells, hESCs) were purchased from WiCell (WA09) and differentiated into human brain organoids. Before organoid generation, hESCs were cultured in a feeder-dependent manner and in a feeder-independent manner following the manufacturer's instructions. For the feeder-dependent culture, mouse embryonic fibroblast (MEF) cells (gifted by Prof. Dr. Servet Ozcan, GENKOK, Kayseri) were cultured on 0.1% gelatin-coated plates with high-glucose DMEM supplemented with 55 µM 2-mercaptoethanol, 1% nonessential amino acids (NEAA), 10% fetal bovine serum (FBS), and 1% penicillin/streptomycin. After the cells reached approximately 80% confluency, they were passaged at a 1:3 to 1:6 ratio using 0.05% trypsin/EDTA. A confluent well of MEFs was mitotically inactivated (called iMEFs) with 10 µg/ml mitomycin C at 37°C for 2.5–3 hours. The cells were washed with 1X phosphate-

buffered saline (PBS) several times, and a vial of H9 cells was thawed from the iMEFs. The cells were cultured with hESC medium (DMEM/F12 containing 2.5 mM L-glutamine, 20% knockout serum (KSR), 55 µM 2-mercaptoethanol, 1% NEAA, 4 ng/mL basic fibroblast growth factor (bFGF) and 10 µM ROCK inhibitor. After colonies were easily visible under a microscope, feeder-independent culture started. In the culture, the colonies were passaged via 0.5 mM EDTA and detached by spraying with mTeSR™1 (Stem Cell Technologies, #85850), after which they were split into growth factor-reduced Matrigel-coated (83 µg/well) 6-well plates. The culture medium, mTeSR™1, was half-replaced every day until the colony confluency reached approximately 70–80%.

Myelinating human brain organoid generation:

The myelinating brain organoids were generated following the previously published protocols with minor modifications (15,18,19). A confluent well of hESCs was incubated with 0.5 mM EDTA and then with Accutase for 4 minutes at room temperature. The colonies were detached from the plate surface by spraying them with low-bFGF medium (DMEM/F12 containing 20% KOSR, 3% heat-inactivated hESC quality FBS, 1% GlutaMAX, 1% NEAA, and 0.05% 2-mercaptoethanol). The cell number was determined by a hemocytometer, the mixture was centrifuged at 200 × g for 5 min, and the mixture was resuspended in low-bFGF medium containing 4 ng/ml bFGF and 50 µM Y-27632 to split the 9000 cells/150 µl/well into U-bottom 96-well plates. Two days later, on Day 2, half of the medium was replaced with low-bFGF medium, and the size of the cell cluster, called the embryoid body, was monitored. On Day 4 and Day 6, the medium was half-replaced until the diameter of the embryoid bodies reached 500–600 µm. The properly grown embryoid bodies were transferred to a well of an ultralow attachment 24-well plate with neural induction medium (DMEM/F12 supplemented with 1% N2, 1%

GlutaMAX, 1% NEAA, and 1 µg/mL heparin). The medium was half-replaced for 3–4 days. Each neuroepithelial tissue sample was subsequently embedded in 30 µL of Matrigel (Corning® Matrigel® Basement Membrane Matrix, 356234) after 20–30 minutes of polymerization of the tissue–Matrigel complex. The tissues in the Matrigel were incubated with differentiation medium (50% DMEM/F12, 50% neurobasal medium, 0.5% N2 supplement, 1% B27, 0.035% 2-mercaptoethanol, 0.025% insulin, 1% GlutaMAX and 0.05% NEAA) without vitamin A. The medium was replaced after 2 days. Later, the medium was supplemented with vitamin A, and the culture was maintained on an orbital shaker (70 RPM) until maturation was completed. During the first four days of culture on the shaker, no additional growth factors were added. After that, 20 ng/mL BDNF (Merck, GF301) and 20 ng/mL NT-3 (Merck, GF308) for the first 10 days, 10 ng/mL PDGF-AA (Merck, GF142) and 10 ng/mL IGF-1 (Merck, GF306) for the second 10 days, and 40 ng/mL 3,3,5-triiodo-L-thyronine (T3, Sigma, ST2877) and 1 µM ketoconazole (Sigma, K1003) for the third 10 days were added to the culture medium, which included vitamin A.

Induction of the inflammation-like response and fingolimod treatment of mature brain organoids: After the addition of all the growth factors, the organoids were incubated with 100 ng/mL lipopolysaccharide (LPS) in culture medium for 24 hours. Then, approximately half of the organoids were treated with 1.27 µM fingolimod (FTY720) for 60 hours on a shaker. The nontoxic concentrations of fingolimod determined in our previous works were used on organoids (20,21).

RNA isolation, cDNA synthesis and quantitative real-time PCR (qRT–PCR): After LPS induction and fingolimod treatment, 8–11 mature organoids were washed with 1X PBS twice, and each

group was incubated with 1 mL of TRIzol (Sigma, T9424) for 1 hour at +4°C. The manufacturer's protocol was then used to obtain total RNA. Later, cDNA for each group was synthesized via a kit (Abm, G236), and qRT–PCR (Promega GoTaq™ qPCR Master Mix, A6002) was performed. β-actin was used as a housekeeping gene, and the primers used are listed in Table S1 (22,23).

Immunofluorescence (IF) Staining: The organoids (3–4 organoids/treatment group) that were treated with LPS and fingolimod followed by LPS were washed with 1X PBS three times and fixed with 4% paraformaldehyde for 15 minutes at room temperature. The samples were subsequently incubated in 30% sucrose solution for 2–3 days at +4°C and embedded in optimum cutting temperature (OCT) solution to be stored at -80°C until sectioning. Later, 20 µm sections were cut with a cryostat, and the sections were incubated for 30–120 minutes at 56°C. The cryosections were washed with 1X PBS three times, permeabilized with 0.25% Triton-X 100 for 10–15 minutes at room temperature and incubated with 3% bovine serum albumin in permeabilization solution for at least 1 hour at room temperature. The sections were incubated with the properly diluted primary antibodies (anti-CNPase, cat no: sc-166558, dilution ratio:1/100; anti-GFAP, cat no:sc-33673, dilution ratio:1/100; anti-Iba1, cat no:sc-32725, dilution ratio:1/150; anti-MBP, cat no:sc-271524, dilution ratio:1/200; anti-SATB2, cat no:sc-518006, dilution ratio:1/150; anti-Sox2, cat no:sc-365823, dilution ratio:1/100; anti-Tau, cat no:sc-390476, dilution ratio:1/100) overnight at +4°C. After the incubation was complete, the sections were washed with 1X PBS three times and incubated with 300 nM 4',6-diamidino-2-phenylindole (DAPI). The sections were imaged under a Leica DM6 B microscope, and the images were analysed via ImageJ (Fiji Version 1.8.0).

Table S1: Gene-specific primer sequences and their annealing (T_m) temperatures

Genes	Forward Primer	Reverse Primer	T_m (°C)
CNPase	CGTGCTGCATTGCACAACCAAG	CTTGCGTGTACAAAAGAGGGCA	61
FOXP3	GTGGCCCGGATGTGAGAAG	GGAGCCCTTGTCTGGATGATG	62
GFAP	GTGTCAGAAAGGCCACCTCAA	TCAGGTCTGGGGAAATGTGC	62
PLP1	GAAAGCCCTTTTCATTGCAGGA	GGCTAGTCTGCTTTGTGGCT	56
β-actin	GCCGCCAGCTCACCAT	GATGCCTCTCTTGCTCTGGG	59

Table S2: Primary antibodies used for immunofluorescence staining

Antibody	Brand	Catalogue No	Dilution
Anti-CNPase	Santa Cruz	sc-166558 AF488	1:100
Anti-GFAP	Santa Cruz	sc-33673 AF594	1:100
Anti-Iba1	Santa Cruz	sc-32725 AF594	1:150
Anti-MBP	Santa Cruz	sc-271524 AF488	1:200
Anti-SATB2	Santa Cruz	sc-518006 AF647	1:150
Anti-Sox2	Santa Cruz	sc-365823 AF488	1:100
Anti-Tau	Santa Cruz	sc-390476 AF488	1:100

Statistical analysis: The images were processed on Fiji v1.54p. The results of the quantitative analysis are presented as the means \pm standard deviations (SDs) and were visualized with GraphPad (Windows version). Comparisons between two groups were performed via one-way ANOVA, followed by Šidák's test. Statistical significance was defined as $p < 0.5$.

Result

Myelinating and mature human brain organoids: Human brain organoids were differentiated from hESCs. The culture of hESCs required both feeder-dependent and feeder-independent cultures. Therefore, H9 cells were first cultured on mitotically inactivated MEFs (Figure 1A and B). After distinct colonies were observed within 9–10 days, they were transferred to growth factor-reduced Matrigel-coated plates. The colonies were cultured for 1–2 passages to remove all MEFs from the culture

environment, and pure hESC colonies were observed (Figure 1C and D). When the colony confluency reached approximately 70–80% of the well, the organoid generation process was started. In the first step, hESC colonies were clustered in a U-bottom 96-well plate, and embryoid bodies (Figure 1E) were obtained within 4–6 days. The debris around the embryoid body and the brightening of the embryoid body surface with smooth edges were expected to have healthy morphologies (19,24), and only the embryoid bodies were transferred to the next step. After their diameters were approximately 500–600 μ m, they were transferred to neural induction medium with a sterile cut 200 μ L pipette tip, not to disturb their morphology. An optically clear and radially organized tissue morphology was observed (Figure 1F). After the optically translucent smooth edges became clearer, the tissues were embedded in an extracellular matrix (Matrigel) and transferred to neural differentiation

medium. Transition between differentiation stages was guided by established morphological cues and the expression of developmental markers, as described in previously validated protocols (15,19,25). These qualitative criteria—such as the appearance of neural rosettes, tissue opacity, and overall organoid

structure—remain standard in brain organoid methodologies and provide reliable indicators of developmental progression. Until mature myelinating organoids were obtained, the developmental process from day 11 to day 50 (Figure 1G-L) was guided by the addition of growth factors.

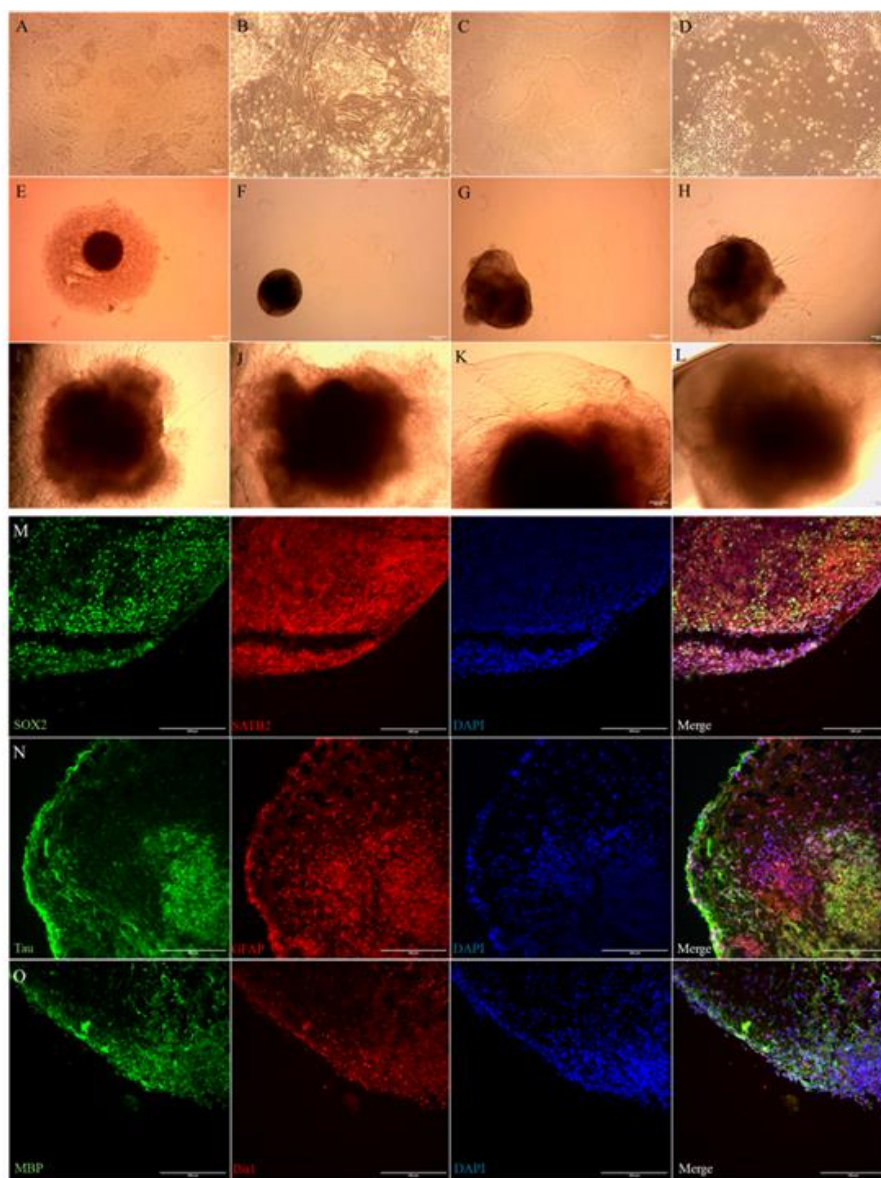


Figure 1. Morphological changes in organoid generation processes from the stem cell stage to mature organoids and characterization of mature organoids. (A-L) Light microscopy images of morphological changes in cells from the stem cell stage to the organoid stage. Feeder-dependent culture of hESCs on iMEFs at (A) 40X and (B) 100X magnification. Feeder-independent culture of hESCs on Matrigel at (C) 40X and (D) 100X magnification. (E) Embryoid body. (F) Ectodermally induced neuroepithelial tissue. Organoids on (G) Day 11, (H) Day 15, (I) Day 22, (J) Day 32, (K) Day 43 and (L) Day 50. Immunofluorescence staining of organoid sections with (M) Sox2 (green) and SATB2 (red) staining, (N) Tau (green) and GFAP (red) staining, and (O) MBP (green) and Iba1 (red) staining. Images A-L and M-O were taken with a Zeiss Primovert and Leica DM6, respectively. Scale bar: 200 µm.

Characterization of myelinating human brain organoids: After the organoids matured within 50–60 days, immunofluorescence staining was performed to reveal their neuronal content. First, a member of the Sry-related HMG box B1 subgroup protein (SOX2), which is used to mark stem cells (26), and SATB2, which is used to mark the excitatory neuron population (27,28), were controlled on organoid cryosections. Figure 1M shows that even though there is a small population of cells with stem cell characteristics, a large portion of the population consists of excitatory neurons. Later, astrocytes with glial fibrillary acid protein (GFAP) and microglia with ionized calcium binding adaptor molecule one (Iba1) (27,29,30) were identified (Figure 1N and O). In addition to the astrocyte and microglial populations, myelinating cells were also detected with the myelin basic protein (MBP) marker in cryosections (Figure 1O) (16,31).

Inflammation model generation by LPS induction: Inflammation-like responses were induced by treatment with 100 ng/mL LPS for 60 hours. The LPS-induced organoids were analysed at the protein level. Immunofluorescence staining revealed a decrease in 2',3'-cyclic nucleotide 3' phosphodiesterase (CNPase)-positive cells, indicating mature/differentiated oligodendrocytes (32,33), and an increase in GFAP-positive cells (27), confirming inflammation in the brain organoids. Figure 2A shows images of marked cryosections stained with GFAP and CNPase, and Figure 2B shows the results of the quantitative analysis, which revealed a statistically

significant decrease in the number of CNPase-positive cells and an approximately 60% increase in the number of GFAP-positive cells.

Fingolimod treatment of LPS-induced organoids: The results in Figure 1 confirmed the generation of mature brain organoids and their neural contents, and the results in Figure 2 confirmed that an inflammation-like response and demyelination was induced after LPS induction by decreasing the number of myelinating cells and increasing the number of astrocytes. After that, one of the commonly used drugs for MS treatment, fingolimod, was tested in brain organoid models, showing a decrease in myelination characteristics and an increase in inflammation characteristics because of LPS induction. Figure 3 shows the effects of fingolimod at the gene and protein levels. A decrease in CNPase and an increase in GFAP-positive cells after LPS induction were associated with a significant increase in CNPase (~2.5-fold) and a significant decrease in GFAP (~10-fold) after fingolimod treatment (Figure 3A and B). To confirm the change in protein levels, relative gene expression levels were measured via qRT-PCR, and Figure 3C shows that the levels of inflammation-related genes (Forkhead box protein P3 (FOXP3)) and GFAP (34,35) were significantly decreased after fingolimod treatment. Even though there was an increase in the relative CNPase (1.6-fold) and PLP1 (1.4-fold) levels, these increases were not statistically significant (Figure 3C).

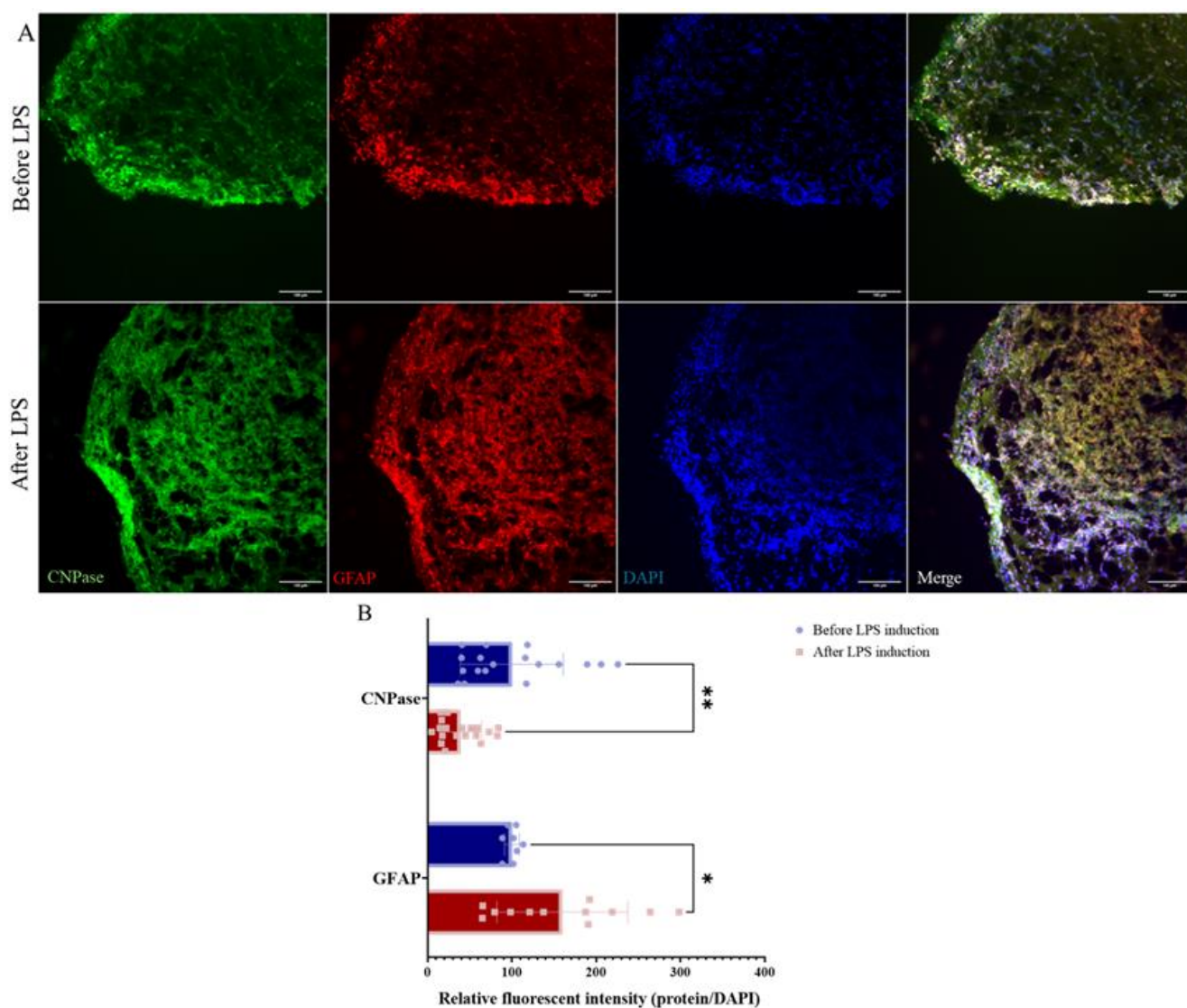


Figure 2. LPS induction of mature organoids. (A) Representative fluorescence images of CNPase and GFAP staining before and after LPS induction. CNPase (green) is a marker for myelination, and GFAP (red) is a marker for neuroinflammation. (B) Quantitative analysis of CNPase and GFAP staining in the LPS-induced and uninduced organoids. Three to four organoids from each group, 10–12 cryosections from each organoid, and 6–7 regions from each cryosection were analysed. The relative fluorescence intensity was measured via Fiji v1.54p and normalized to that of DAPI. The graphs were generated with GraphPad Prism 9.0. The data were statistically analysed by one-way ANOVA with Šidák's test (ns $p > 0.05$, * $p < 0.05$, ** $p < 0.01$, *** $p \leq 0.001$, **** $p \leq 0.0001$), and the images were taken with a Leica DM6 B (scale bar: 200 μm).

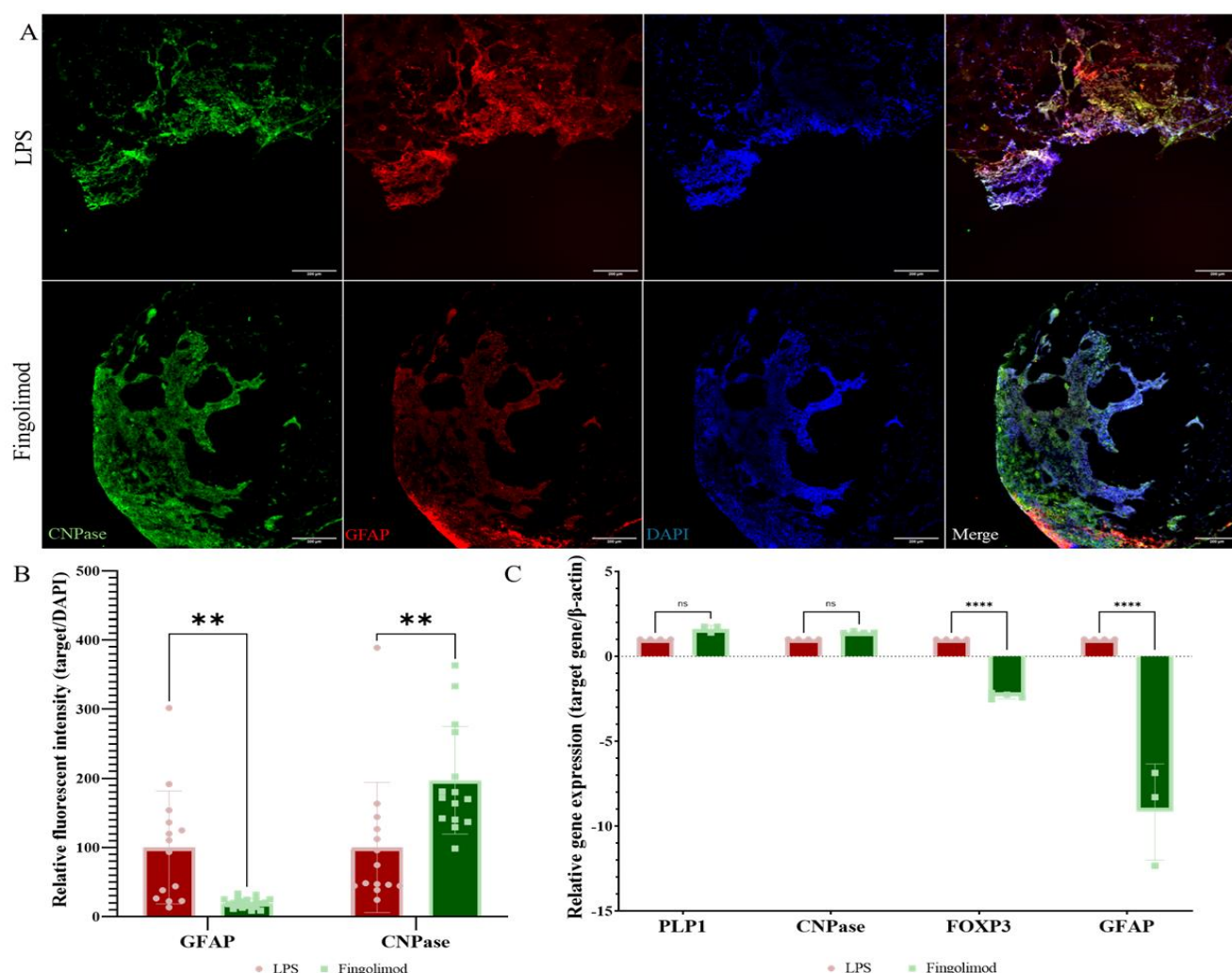


Figure 3. Fingolimod treatment of LPS-induced mature organoids. (A) Representative fluorescence images of CNPase and GFAP staining before and after fingolimod treatment. CNPase (green) is a marker for myelination, and GFAP (red) is a marker for neuroinflammation. (B) Quantitative analysis of CNPase and GFAP staining in the fingolimod-treated and untreated organoids. Three to four organoids from each group, 10 cryosections from each organoid, and 6–7 regions from each cryosection were analysed. The relative fluorescence intensity was measured via Fiji v1.54p and normalized to that of DAPI. (C) Changes in relative gene expression levels after fingolimod treatment compared with LPS induction. Myelination-related transcript levels (PLP1 and CNPase) and inflammation-related transcript levels (FOXP3 and GFAP) were measured via qRT-PCR. The graphs were generated with GraphPad Prism 9.0. The data were statistically analysed by one-way ANOVA with Šidák's test (ns $p > 0.05$, * $p < 0.05$, ** $p < 0.01$, *** $p \leq 0.001$, **** $p \leq 0.0001$), and the images were taken with a Leica DM6 B (scale bar: 200 μ m).

Discussion

Multiple sclerosis is an immune-mediated neurodegenerative disease that causes demyelination in the central nervous system and affects more than 2.5 million people worldwide. Although it is known to be a T-cell-mediated autoimmune disease, its immunopathology has not been fully explored (1). Most

of the knowledge about disease pathogenesis comes from animal models, including experimental autoimmune/allergic encephalomyelitis (EAE) models for studying autoimmune pathogenesis, Theiler's murine encephalomyelitis virus (TMEV) infection model and toxin-induced demyelination models for

studying axonal repair and remyelination processes (22,36,37). Because of the limitations of the currently used MS models, a new model must be improved. Since there is no single animal model that reflects all aspects of human MS pathogenesis, especially inbred mouse strains, which are characterized by genetic irregularities, and especially the immune systems of rodents and humans, which are profoundly different, the use of animal models is not a perfect tool for studying MS (36,38). In addition to animal models, 2D culture models have unquestionably disadvantages. Unlike the ease of cell line maintenance, relatively low cost, and homogenous exposure to stimuli, these methods have major disadvantages, including a lack of cell–cell and cell–environment interactions, cell polarity dynamics and cell type heterogeneity, and 2D cultures are not good models for studying MS (38,39). The need for cell–cell and cell–environment complexity mimicking a heterogeneous cell type niche has led to the development of new tools to study disease pathology (38). Brain organoids are three-dimensional (3D) culture models created from either embryonic stem cells or pluripotent stem cells to differentiate brain tissue-like structures under the guidance of the extracellular matrix and growth factors (8,40). One study reported that the organoids generated from pluripotent stem cells are useful tools for studying MS (12,38); however, current brain organoid generation protocols may not be preferable because of the experimental duration (~210 days) and the lack of heterogeneity in microglial physiology (15,16). Considering the necessity of brain organoids to reflect MS and the disadvantages of previously published protocols, we optimized human brain organoid generation in this study and reported their usage in the drug screening field.

First, unlike the previously published protocol, which involves generating organoids in 30 weeks in dynamic culture (15), maturation was completed in 50–60 days

by addition of bFGF at the embryoid body stage and heparin at the neural induction stage in this study. Because bFGF has a function to sustain neural progenitor cell proliferation (41) and heparin functions in neural communication and brain development (42) providing neurotrophic factor binding ability (43). Figure 1A-L shows that cell and tissue morphology changes from the stem cell stage to the mature organoid stage. At the stem cell stage, the iMEFs and growth factor-reduced Matrigel were cultured in feeder-dependent and feeder-independent manners, respectively. When the center of the colonies was in the dark or the edges of the colonies were moving closer, they were passaged or moved to the next step. The micrographs of healthy stem cell colonies are shown in Figure 1A and C. Figure 1E-L shows the progression of tissue development. During development, the instructions of previously published protocols were logically combined with minor changes (15,19). As expected, radially organized ectodermal induction with brighter edges (Figure 1F) and budding structures with minor outgrowth (Figure 1H-I) were observed during development (19). After morphology-based confirmation, the organoids were cryosectioned and immunostained with fluorescently labelled antibodies to label stem cells with SOX2, an excitatory neural cell population with SATB2 (Figure 1M) (26-28), neuronal cell characteristics indicating axons with Tau, astrocytes with GFAP (Figure 1N) (27,29,30,44), a microglial population with Iba1 and a myelinating cell population with MBP (Figure 1O) (16,29,31). The previously published protocols indicate that one of the disadvantages of brain organoids in modelling neurodegenerative diseases is the lack of microglia (45), and one of the common pathologies in MS is microglial activation, which leads to increased neurodegeneration (1). Considering these findings, a promising improvement is that the organoids had a microglial cell population in this study (Figure 1O). Moreover, a small population of adult stem cells with a

large population of mature neuron types, astrocytes, microglia, and myelinating cells were found in our organoids. After cell population heterogeneity was confirmed by immunostaining, MS modelling of the organoids was performed with LPS, which induces demyelination and inflammation (46). In support of the literature, the percentage of myelinating cells, which were marked by CNPase, was significantly decreased, and the astrocyte population was significantly increased after induction (Figure 2A and B). This finding indicates that the model mimics the inflammation- and demyelination-related pathogenesis of MS. Last, the use of organoids in MS treatment-related studies is needed. Since brain organoids have great potential for neurodegenerative disease-related drug screening studies (47), our organoid models were tested in terms of treatability. Fingolimod was the first oral treatment approved in 2009 by the Food and Drug Administration (FDA) (1). The treatment effect of fingolimod has already been proven in the literature (48,49). Therefore, in this study, its positive effect on MS-generated human brain organoids was revealed at the protein and gene levels. Figure 3A and its quantitative analysis results in Figure 3B show that myelination was increased and inflammation was decreased after fingolimod treatment. It is possible that 80% of GFAP-positive cells were decreased and that more than 90% of CNPase-positive cells were increased. The relative gene expression change was then quantitatively measured via qRT-PCR. The levels of PLP1 and CNPase were not significantly increased; however, the levels of inflammatory markers (GFAP and FOXP3) were significantly decreased after fingolimod treatment. This is also a predictable result because all organoid


architectures, including the inner core and outer core structures, are highly heterogeneous. As expected, as shown in Figure 1N-O, even though the presence of inflammation- and myelination-related cells was not homogenous on the organoid section plane and immunostaining detected only the spatially restricted area, qRT-PCR was used to measure the transcripts of all the cell types in the organoid. Therefore, since myelinating cells were prominent around the outer core of the organoid sections (Figure 1O, 2A and 3A), the qRT-PCR results may not reveal a significant increase in myelination markers, unlike immunostaining. However, overall, the results demonstrated that when myelinating organoids with a heterogeneous cell population were generated, they were able to be used for MS modelling, and model treatability was tested via fingolimod.


Author Contribution: AS and BA conceptualized and designed the study. Data collection for 2D and 3D cell culture experiments, IF staining, and qRT-PCR were performed by BA. BA drafted the manuscript and prepared the figures. AS revised the manuscript. All the authors have thoroughly examined and endorsed the final version of the manuscript.

Funding: This work was supported by grants from the Scientific and Technological Research Council of Türkiye (TUBITAK 119Z389).

Declaration : No potential conflict of interest relevant to this article was reported.

ORCID

Büşra Acar  0000-0002-4772-2698

Alaattin Şen  0000-0002-8444-376X

References

1. Gironi M, Arnò C, Comi G, Penton-Rol G, Furlan R. Chapter 4 - Multiple Sclerosis and Neurodegenerative Diseases. In: Boraschi D, Penton-Rol G, editors. Immune Rebalancing: Academic Press; 2016. p. 63–84.
2. Sheikh S, Safia, Haque E, Mir SS. Neurodegenerative Diseases: Multifactorial Conformational Diseases and Their Therapeutic Interventions. J Neurodegener Dis 2013;2013:563481.

3. Liu Z, Liao Q, Wen H, Zhang Y. Disease modifying therapies in relapsing-remitting multiple sclerosis: A systematic review and network meta-analysis. *Autoimmun Rev* 2021;20:102826.
4. Ferret-Sena V, Capela C, Macedo A, Salgado AV, Derudas B, Staels B, et al. Fingolimod treatment modulates PPARgamma and CD36 gene expression in women with multiple sclerosis. *Front Mol Neurosci* 2022;15:1077381.
5. Roy R, Alotaibi AA, Freedman MS. Sphingosine 1-Phosphate Receptor Modulators for Multiple Sclerosis. *CNS Drugs* 2021;35:385–402.
6. Kukanja P, Langseth CM, Rubio Rodriguez-Kirby LA, Agirre E, Zheng C, Raman A, et al. Cellular architecture of evolving neuroinflammatory lesions and multiple sclerosis pathology. *Cell* 2024;187:1990–2009 e19.
7. Urrestizala-Arenaza N, Cerchio S, Cavaliere F, Magliaro C. Limitations of human brain organoids to study neurodegenerative diseases: a manual to survive. *Front Cell Neurosci* 2024;18:1419526.
8. Kim J, Koo BK, Knoblich JA. Human organoids: model systems for human biology and medicine. *Nat Rev Mol Cell Biol* 2020;21:571–84.
9. Scuderi S, Altobelli GG, Cimini V, Coppola G, Vaccarino FM. Cell-to-Cell Adhesion and Neurogenesis in Human Cortical Development: A Study Comparing 2D Monolayers with 3D Organoid Cultures. *Stem Cell Reports* 2021;16:264–80.
10. Bose R, Banerjee S, Dunbar GL. Modeling Neurological Disorders in 3D Organoids Using Human-Derived Pluripotent Stem Cells. *Front Cell Dev Biol* 2021;9:640212.
11. Yan Y, Song L, Bejoy J, Zhao J, Kanekiyo T, Bu G, et al. Modeling Neurodegenerative Microenvironment Using Cortical Organoids Derived from Human Stem Cells. *Tissue Eng Part A* 2018;24:1125–37.
12. Daviaud N, Chen E, Edwards T, Sadiq SA. Cerebral organoids in primary progressive multiple sclerosis reveal stem cell and oligodendrocyte differentiation defect. *Biol Open* 2023;12.
13. Simoes-Abade MBC, Patterer M, Nicaise AM, Pluchino S. Brain organoid methodologies to explore mechanisms of disease in progressive multiple sclerosis. *Front Cell Neurosci* 2024;18:1488691.
14. Chen X, Sun G, Feng L, Tian E, Shi Y. Human iPSC-derived microglial cells protect neurons from neurodegeneration in long-term cultured adhesion brain organoids. *Commun Biol* 2025;8:30.
15. Madhavan M, Nevin ZS, Shick HE, Garrison E, Clarkson-Paredes C, Karl M, et al. Induction of myelinating oligodendrocytes in human cortical spheroids. *Nat Methods* 2018;15:700–6.
16. Shaker MR, Pietrogrande G, Martin S, Lee JH, Sun W, Wolvetang EJ. Rapid and Efficient Generation of Myelinating Human Oligodendrocytes in Organoids. *Front Cell Neurosci* 2021;15:631548.
17. Bodnar B, Zhang Y, Liu J, Lin Y, Wang P, Wei Z, et al. Novel Scalable and Simplified System to Generate Microglia-Containing Cerebral Organoids From Human Induced Pluripotent Stem Cells. *Front Cell Neurosci* 2021;15:682272.
18. Acar B, Aktas-Pepe N, Sen A. Optimization of myelination on human cerebral organoids for studying multiple sclerosis (MS). *The EuroBiotech Journal* 2021;5:58.
19. Lancaster MA, Knoblich JA. Generation of cerebral organoids from human pluripotent stem cells. *Nat Protoc* 2014;9:2329–40.
20. Aktas Pepe N, Acar B, Erturk Zararsiz G, Ayaz Guner S, Sen A. Role of Long Non-Coding RNA X-Inactive-Specific Transcript (XIST) in Neuroinflammation and Myelination: Insights from Cerebral Organoids and Implications for Multiple Sclerosis. *Non-Coding RNA* 2025;11:31.
21. Turgut G, Doyduk D, Yildırım Y, Yavuz S, Akdemir A, Dişli A, et al. Computer design, synthesis, and bioactivity analyses of drugs like fingolimod used in the treatment of multiple sclerosis. *Bioorg Med Chem* 2017;25:483–95.
22. Ozgun-Acar O, Celik-Turgut G, Gazioglu I, Kolak U, Ozbal S, Ergur BU, et al. Capparid ovata treatment suppresses inflammatory cytokine expression and ameliorates experimental allergic encephalomyelitis model of multiple sclerosis in C57BL/6 mice. *J Neuroimmunol* 2016;298:106–16.
23. Ucar Akyurek T, Orhan IE, Senol Deniz FS, Eren G, Acar B, Sen A. Evaluation of Selected Plant Phenolics via Beta-Secretase-1 Inhibition, Molecular Docking, and Gene Expression Related to Alzheimer's Disease. *Pharmaceuticals (Basel)* 2024;17.
24. Sutcliffe M, Lancaster MA. A Simple Method of Generating 3D Brain Organoids Using Standard Laboratory Equipment. *Methods Mol Biol* 2019;1576:1–12.
25. Qian X, Nguyen HN, Song MM, Hadiono C, Ogden SC, Hammack C, et al. Brain-Region-Specific Organoids Using Mini-bioreactors for Modeling ZIKV Exposure. *Cell* 2016;165:1238–54.
26. Novak D, Huser L, Elton JJ, Umansky V, Altevogt P, Utikal J. SOX2 in development and cancer biology. *Semin Cancer Biol* 2020;67:74–82.
27. Fu H, Possenti A, Freer R, Nakano Y, Hernandez Villegas NC, Tang M, et al. A tau homeostasis signature is linked with the cellular and regional vulnerability of excitatory neurons to tau pathology. *Nat Neurosci* 2019;22:47–56.
28. Huang Y, Song NN, Lan W, Hu L, Su CJ, Ding YQ, et al. Expression of transcription factor Satb2 in adult mouse brain. *Anat Rec (Hoboken)* 2013;296:452–61.
29. Bartalska K, Hubschmann V, Korkut-Demirbas M, Cubero RJA, Venturino A, Rossler K, et al. A systematic characterization of microglia-like cell occurrence during retinal organoid differentiation. *iScience* 2022;25:104580.
30. Walsh RM, Luongo R, Giacomelli E, Ciceri G, Rittenhouse C, Verrillo A, et al. Generation of human cerebral organoids with a structured outer subventricular zone. *Cell Rep* 2024;43:114031.
31. Matsui TK, Matsubayashi M, Sakaguchi YM, Hayashi RK, Zheng C, Sugie K, et al. Six-month cultured cerebral organoids from human ES cells contain matured neural cells. *Neurosci Lett* 2018;670:75–82.
32. Nascimento JM, Saia-Cereda VM, Sartore RC, da Costa RM, Schitine CS, Freitas HR, et al. Human Cerebral Organoids and Fetal Brain Tissue Share Proteomic Similarities. *Front Cell Dev Biol* 2019;7:303.
33. Verrier JD, Jackson TC, Gillespie DG, Janesko-Feldman K, Bansal R, Goebbels S, et al. Role of CNPase in the oligodendrocytic extracellular 2',3'-cAMP-adenosine pathway. *Glia* 2013;61:1595–606.
34. Phe V, Roupert M, Cussenot O, Chartier-Kastler E, Game X, Comperat E. Forkhead box protein P3 (Foxp3) expression serves as an early chronic inflammation marker of squamous cell differentiation and aggressive pathology of urothelial carcinomas in neurological patients. *BJU Int* 2015;115 Suppl 6:28–32.
35. von Boyen GB, Steinkamp M, Reinshagen M, Schafer KH, Adler G, Kirsch J. Proinflammatory cytokines increase glial fibrillary acidic protein expression in enteric glia. *Gut* 2004;53:222–8.
36. Procaccini C, De Rosa V, Pucino V, Formisano L, Matarese G. Animal models of Multiple Sclerosis. *Eur J Pharmacol* 2015;759:182–91.
37. Senol H, Ozgun-Acar O, Dag A, Eken A, Guner H, Aykut ZG, et al. Synthesis and Comprehensive in Vivo Activity Profiling of Olean-12-en-28-ol, 3beta-Pentacosanoate in Experimental Autoimmune Encephalomyelitis: A Natural Remyelinating and Anti-Inflammatory Agent. *J Nat Prod* 2023;86:103–18.
38. Czapkowska J, Kaluza M, Szpakowski P, Glabinski A. An Overview of Multiple Sclerosis In Vitro Models. *Int J Mol Sci* 2024;25.
39. Kapalczyńska M, Kolenda T, Przybyła W, Zajaczowska M, Teresiak A, Filas V, et al. 2D and 3D cell cultures - a comparison of different types of cancer cell cultures. *Arch Med Sci* 2018;14:910–9.
40. Heo JH, Kang D, Seo SJ, Jin Y. Engineering the Extracellular Matrix for Organoid Culture. *Int J Stem Cells* 2022;15:60–9.
41. Gu L, Cai H, Chen L, Gu M, Tchieu J, Guo F. Functional Neural Networks in Human Brain Organoids. *BME Front* 2024;5:0065.
42. Yan Y, Bejoy J, Marzano M, Li Y. The Use of Pluripotent Stem Cell-Derived Organoids to Study Extracellular Matrix Development during Neural Degeneration. *Cells* 2019;8.
43. Bejoy J, Wang Z, Bijonowski B, Yang M, Ma T, Sang QX, et al. Differential Effects of Heparin and Hyaluronic Acid on Neural Patterning of Human Induced Pluripotent Stem Cells. *ACS Biomater Sci Eng* 2018;4:4354–66.

44. Kanaan NM, Grabinski T. Neuronal and Glial Distribution of Tau Protein in the Adult Rat and Monkey. *Front Mol Neurosci* 2021;14:607303.
45. Chen X, Sun G, Tian E, Zhang M, Davtyan H, Beach TG, et al. Modeling Sporadic Alzheimer's Disease in Human Brain Organoids under Serum Exposure. *Adv Sci (Weinh)* 2021;8:e2101462.
46. Felts PA, Woolston AM, Fernando HB, Asquith S, Gregson NA, Mizzi OJ, et al. Inflammation and primary demyelination induced by the intraspinal injection of lipopolysaccharide. *Brain* 2005;128:1649–66.
47. Giorgi C, Lombardozzi G, Ammannito F, Scenna MS, Maceroni E, Quintiliani M, et al. Brain Organoids: A Game-Changer for Drug Testing. *Pharmaceutics* 2024;16.
48. Aytan N, Choi JK, Carreras I, Brinkmann V, Kowall NW, Jenkins BG, et al. Fingolimod modulates multiple neuroinflammatory markers in a mouse model of Alzheimer's disease. *Sci Rep* 2016;6:24939.
49. Zhang Y, Li X, Ciric B, Ma CG, Gran B, Rostami A, et al. Effect of Fingolimod on Neural Stem Cells: A Novel Mechanism and Broadened Application for Neural Repair. *Mol Ther* 2017;25:401–15.